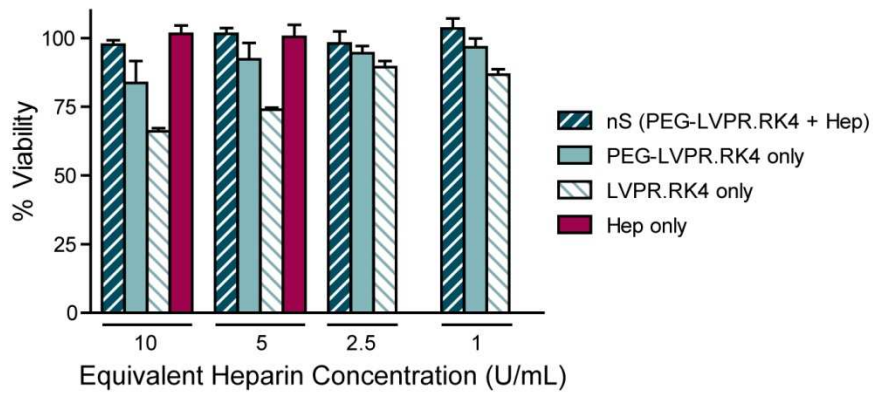


## Supporting Information

# Self-titrating Anticoagulant Nanocomplexes That Restore Homeostatic Regulation of the Coagulation Cascade

Kevin Y. Lin<sup>1</sup>, Justin H. Lo<sup>2,3</sup>, Nikita Consul<sup>1</sup>, Gabriel A. Kwong<sup>2</sup>, and Sangeeta N. Bhatia<sup>2,4,5,6,\*</sup>

<sup>1</sup>Department of Chemical Engineering, Massachusetts Institute of Technology, Cambridge, MA 02139; <sup>2</sup>Harvard-MIT Division of Health Sciences and Technology, Massachusetts Institute of Technology, Cambridge, MA 02139; <sup>3</sup>Medical Scientist Training Program, Harvard Medical School, Boston, MA 02115; <sup>4</sup>Broad Institute of Harvard and MIT, Cambridge, MA 02142; <sup>5</sup>Department of Medicine, Brigham and Women's Hospital, Boston, MA 02115; <sup>6</sup>Electrical Engineering and Computer Science, David H. Koch Institute for Integrative Cancer Research, MIT, Cambridge, MA 02139; <sup>7</sup>Howard Hughes Medical Institute, Chevy Chase, Maryland 20815, USA.



**Figure S1. Cell viability assay.** Percent viability of HUVECs incubated with varying concentrations of nanoSTATs (nS), PEG-LVPR.RK4, LVPR.RK4, and free heparin as determined by MTS assay (n = 3 per condition).

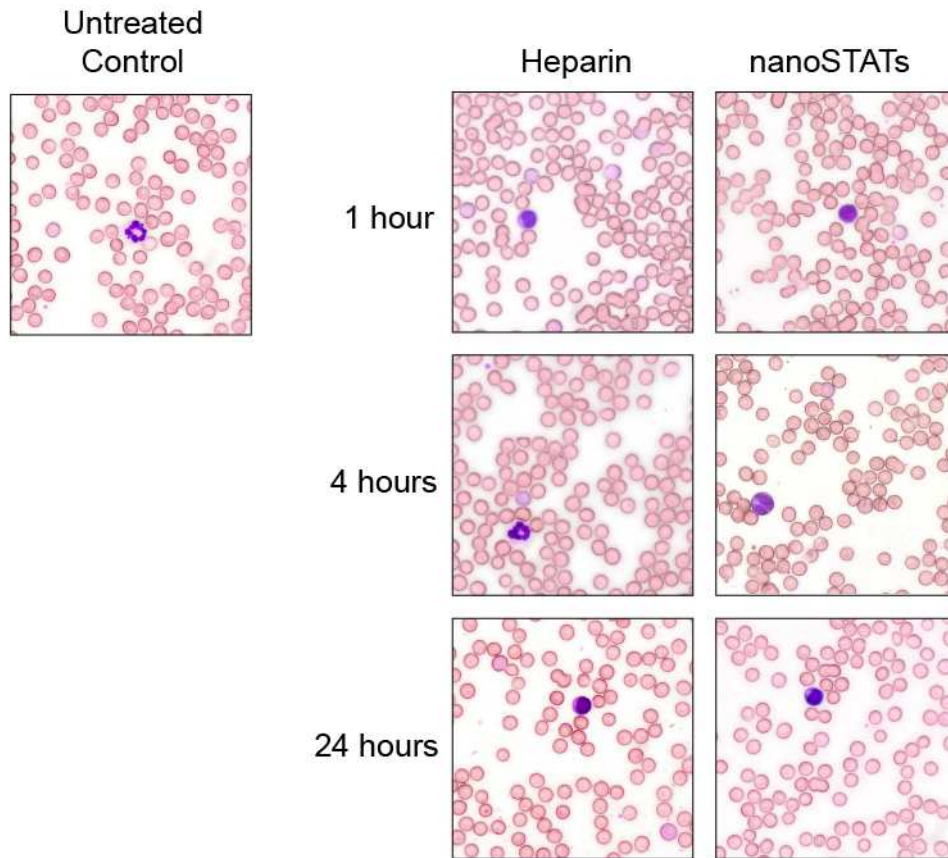


**Figure S2. Blood smears.** Representative imaging of peripheral blood smears (Wright-Giemsa stain) from mice 1, 4, and 24 hours after dosing with either heparin (200 U/kg) or nanoSTATs (200 U/kg equivalent heparin), compared to untreated control.

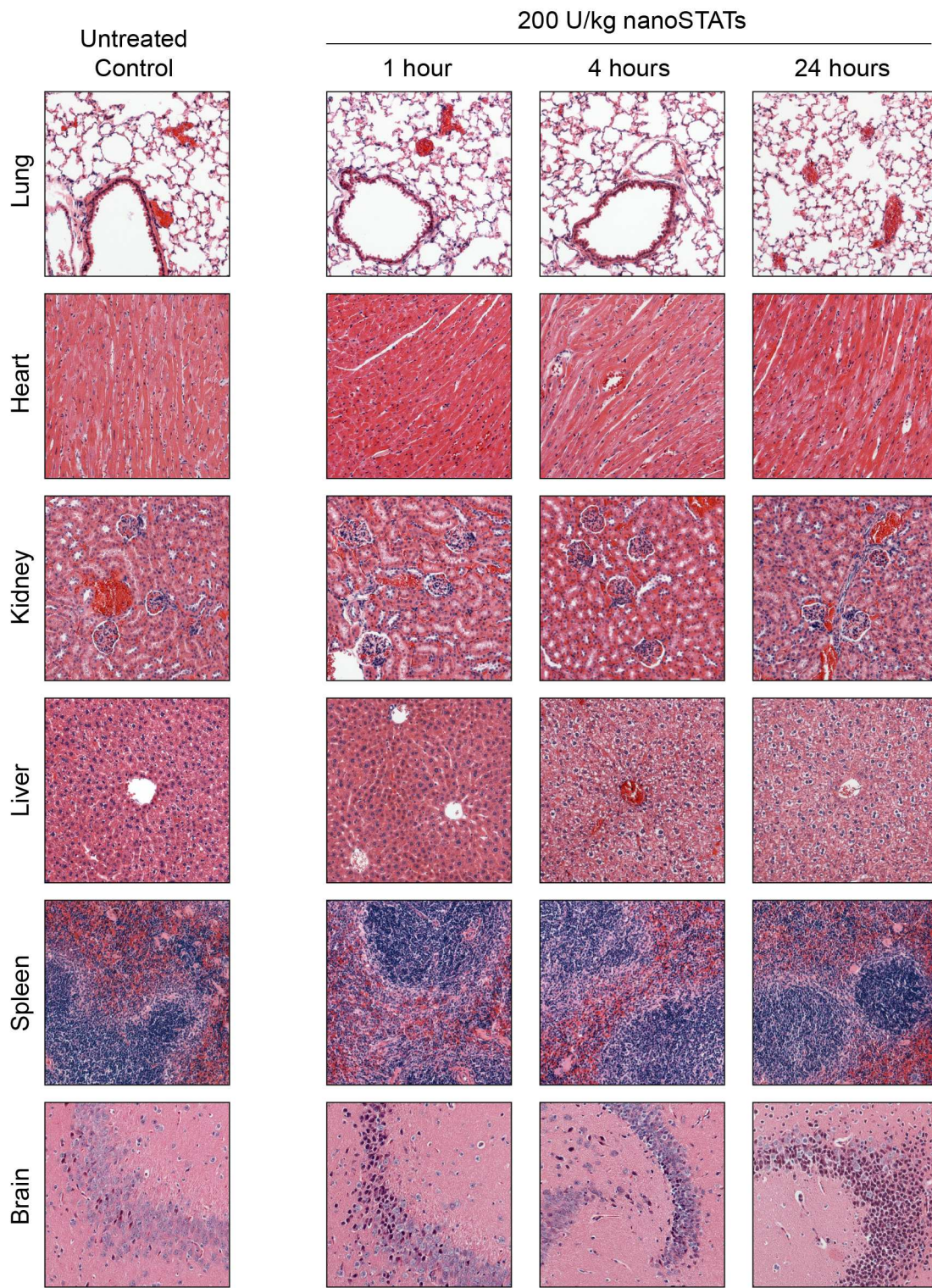


**Figure S3. H&E staining of organs from mice dosed with nanoSTATs.** Lungs, hearts, kidneys, livers, spleens, and brains from mice 1, 4, and 24 hours after dosing with 200 U/kg nanoSTATs *versus* untreated controls. Scale bar: 100  $\mu$ m.

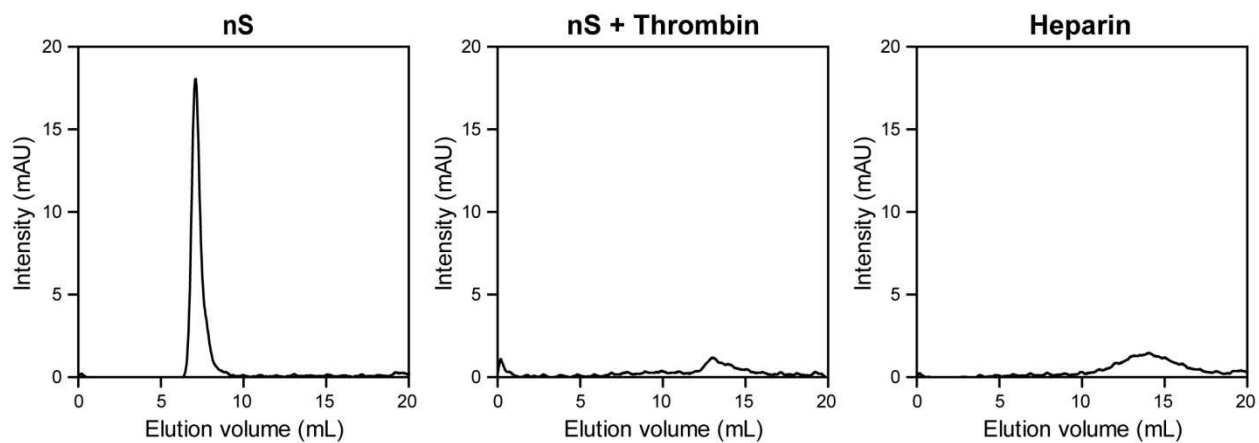


**Figure S4. FPLC analysis of nanoSTATs.** FPLC chromatograms of intact nanoSTATs (nS), nanoSTATs incubated with thrombin, and free heparin as monitored by absorbance at 488 nm.



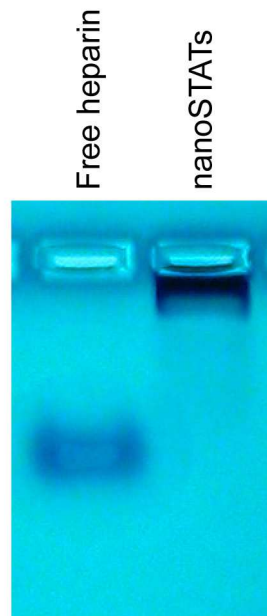


**Figure S5. Electrophoretic gel retardation assay with Alcian Blue stain.** 60  $\mu\text{g}$  free unfractionated heparin (left lane) or nanoSTATs encapsulating 60  $\mu\text{g}$  of heparin (right lane) run on a 1% agarose gel, with heparin stained using Alcian Blue 8GX.

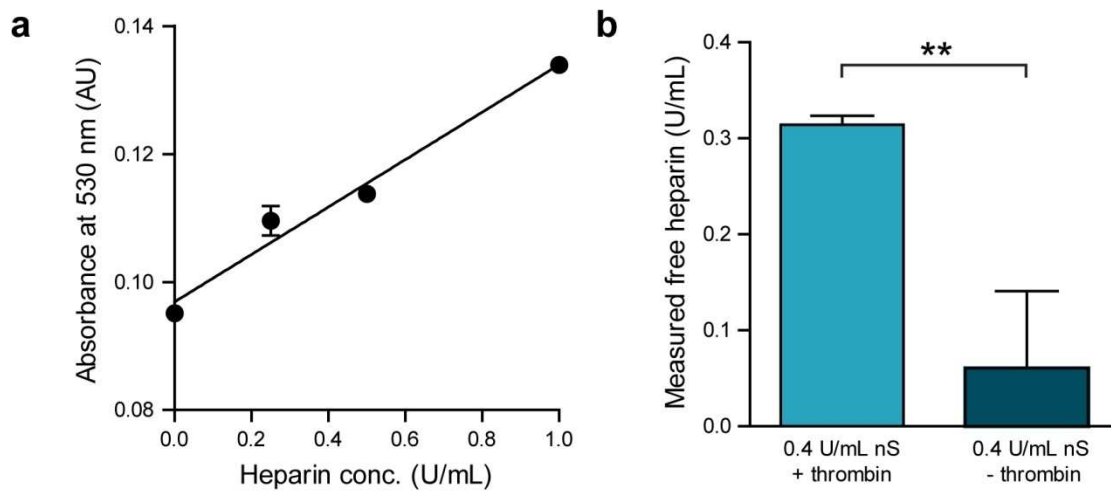


**Figure S6. Azure II assay for heparin quantification.** (a) Standard curve of free heparin mixed with Azure II (slope = 0.037, y-intercept = 0.097,  $r^2 = 0.98$ ;  $n = 3$  per condition, s.d.). (b) Free heparin from nanoSTATs quantified before and after incubation with thrombin by Azure II assay. Absorbance was compared to the standard curve of free heparin from (a) to determine the amount of free heparin (\*\* $P < 0.05$  by Student's  $t$ -test;  $n = 3$  per condition, s.d.).

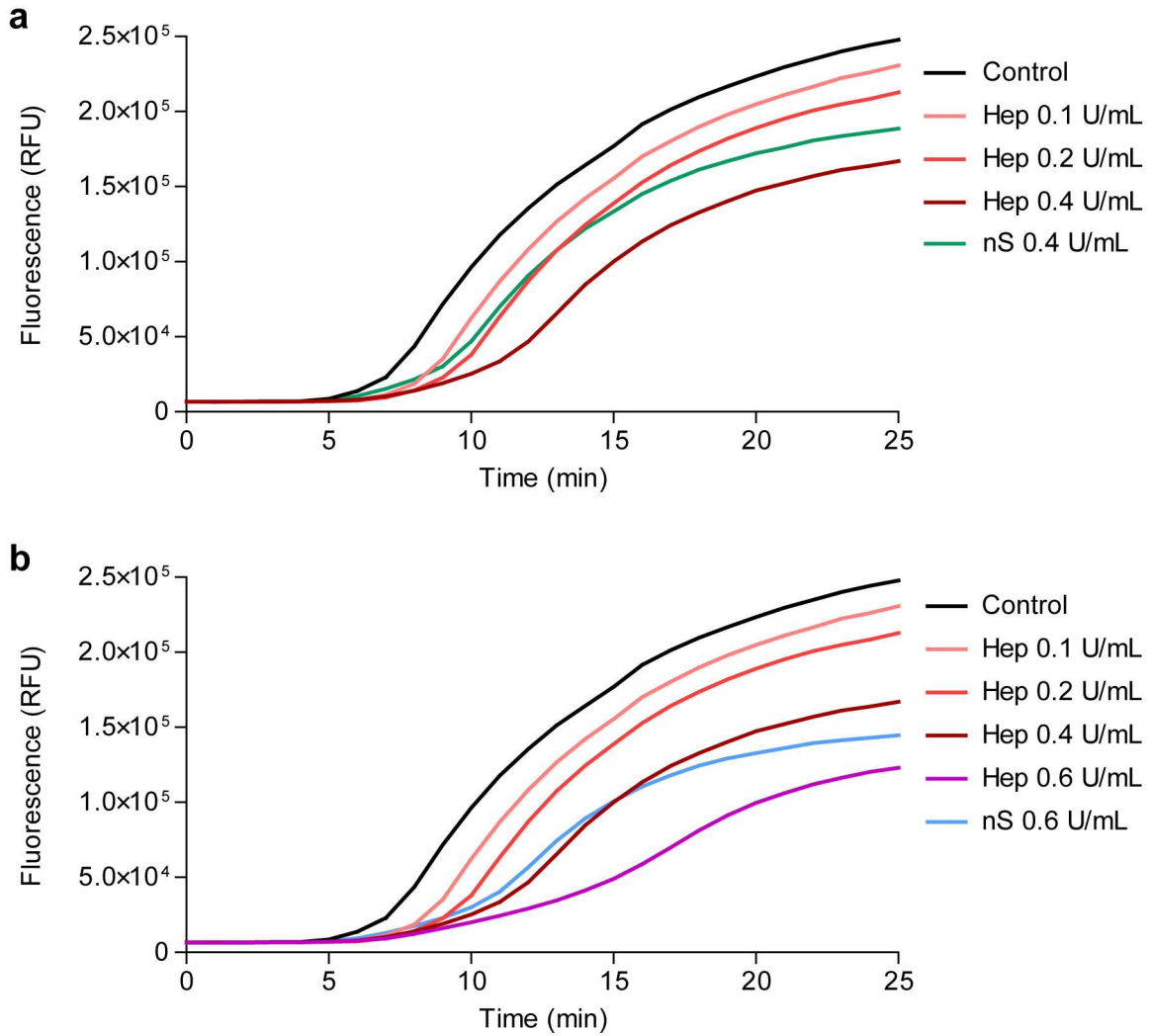


**Figure S7. Fluorescence signal from thrombin generation assay.** Fluorescence traces from cleavage of fluorogenic substrate by thrombin in normal human control plasma spiked with (a) 0.4 U/mL and (b) 0.6 U/mL of nanoSTATs plotted against representative traces from plasma spiked with various concentrations of free heparin ( $n = 3$  per condition; excitation: 360 nm; emission: 460 nm).



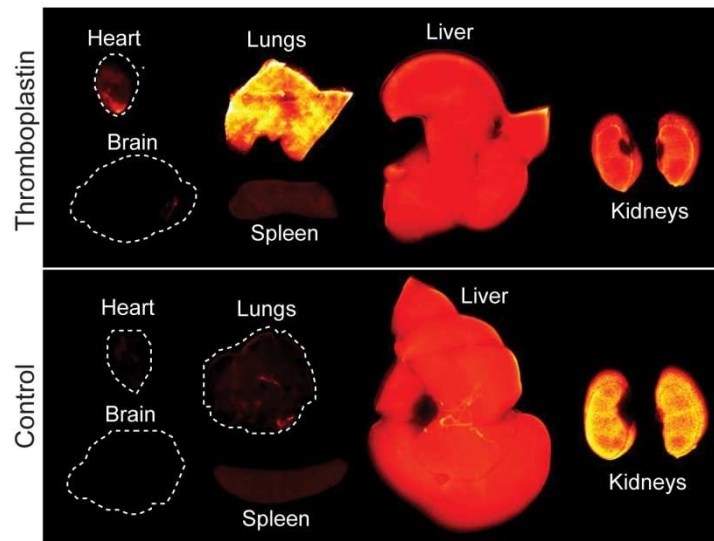


**Figure S8. Deposition of VT750-fibrin in thromboplastin-induced model of thrombosis.** Near-infrared fluorescent scans of excised organs to assess VT750-fibrin distribution following intravenous injection of thromboplastin ( $2 \mu\text{L/g b.w.}$ ) or PBS.

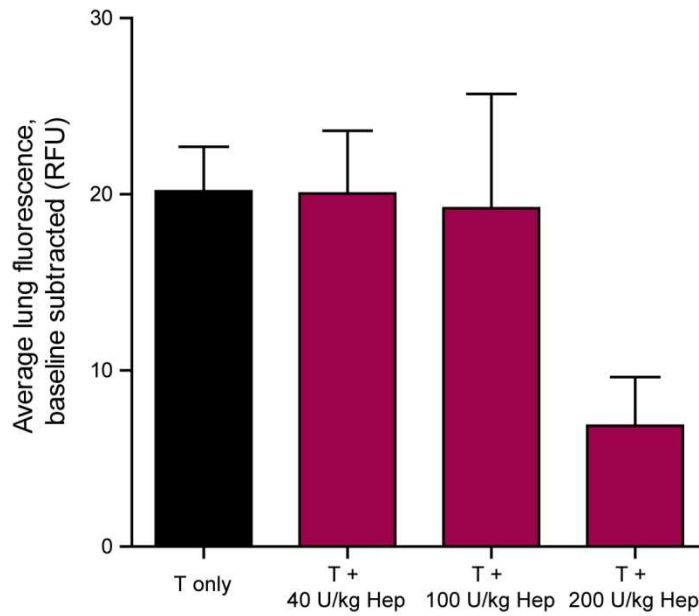


**Figure S9. Heparin dose response in thromboplastin-induced thrombosis model.** Quantification of fibrin deposited in the lungs in response to escalating doses of heparin (Hep) (n = 3–5 mice, s.e.).